



**AIB-VINCOTTE**

FOREST CENTRAL OFFICE

Avenue du Roi, 157 - B-1060 Brussels

Phone (2) 536 82 11 - Telex 22550 - Fax (2) 537 46 19

R&D n° : 47-3-0048-4

March, 94

**BELGIAN UT EVALUATION  
OF THE PISC III AUSTENITIC STAINLESS STEEL SPECIMENS**

**SPECIALISTS MEETING ON NON-DESTRUCTIVE EXAMINATION  
PRACTICE AND RESULTS**

**Petten, The Netherlands, 8-10 March 1994**

**G. MAES, J. CERMAK, B. HANSOUL, G. HENNAUT, Ph. DOMBRET**

# BELGIAN UT EVALUATION OF THE PISC III AUSTENITIC STAINLESS STEEL SPECIMENS

G. Maes, J. Cermak, B. Hansoul, G. Hennaut, Ph. Dombret

AIB-Vincotte (BELGIUM)

## Abstract

Due to their coarse-grain structure, austenitic stainless steels in general, and cast or welded components in particular, can strongly affect the performance of ultrasonic examination techniques.

Within the framework of Action 4 (Austenitic Steel Testing) of the PISC III programme, a number of capability assessment exercises were conducted on test assemblies featuring various types of austenitic material.

This paper discusses the outcome and the experience gained from the Belgian participation in Action 4. Both the detection and sizing capabilities of the applied inspection techniques are evaluated, and the influence of flaw characteristics is investigated. Moreover, specific features of newly developed probes and scanning equipment are illustrated, and their industrial applicability is evaluated.

Finally, guidelines are deduced as to the selection of appropriate UT examination techniques for austenitic stainless steels, in relation with both the geometry and the metallurgical structure of the considered component.

## 1. Introduction

Action 4 of the PISC III programme aimed at assessing the inspection capability of non-destructive evaluation techniques and procedures in austenitic stainless steel components, such as the main coolant piping and the auxiliary piping of light water nuclear reactors.

Capability studies were organised, as round-robin tests, for different types of austenitic steel components : wrought-to-wrought, cast-to-cast, cast-to-wrought. One or more Belgian teams participated in each of these tests.

## 2. W/W Capability Study

### 2.1. Test Specimens

The set of test specimens considered in the wrought-to-wrought capability study consisted of six wrought stainless steel assemblies, each of them containing one weld to inspect. Assemblies 31, 32, 33 and 36 were straight pipes whereas assemblies 34 and 35 presented a curved elbow. The nominal outer diameter was 320 mm for all assemblies, while the wall thickness ranged from 11 to 25 mm. The considered specimens were representative for the auxiliary piping of the Belgian pressurized water nuclear reactors.

The set of intended flaws featured four different types. Assemblies 31, 34 and 35 contained only IGSCC defects. Mechanical as well as thermal fatigue cracks, embedded notches, and EDM notches (PISC type "A" defects) were present in the other assemblies.

A detailed description of the assemblies and the nature and the location of each flaw can be found in (1).

### 2.2. Test Procedures

The Belgian team performed an automated ultrasonic inspection using a field pipe scanning mechanism connected to an in-house data acquisition and processing system.

Contact probes excited at 2 MHz were used. The inspection procedure prescribes both compression wave twin-crystal search units and shear wave transducers, refracted at 45, 60, and 70 degrees in steel.

The local noise level was applied as detection threshold. Where available, tip diffraction signals were used for depth sizing. In all other cases, the 6 dB amplitude drop method was used.

The inspection was limited to the examination of the weld regions of the different assemblies, and only circumferential flaws were searched for.

### 2.3. Flaw Detection Capability

The quantitative assessment of the detection capability of the applied procedure was performed using the standard set of descriptive statistical parameters defined for the PISC III programme (2). The graphs of Figs. 1-4 show the outcome of the exercise for each of the assemblies. Only the flaws within the scope of the Belgian procedure were taken into account. As the number of indications in each assembly was very limited (an average of 3), the influence of a single flaw was sometimes determining for the result.

The applied procedure demonstrated an excellent detection capability: none of the flaws was missed, resulting in an FDF of 100 %. Only 2 false calls were reported. A single false call in assembly 33 yields a FCRD of 100 %. The detection of a 0.4 mm deep, 18 mm long EDM notch in

the HAZ of a 25 mm thick weld, shown on Fig.5, is a good illustration of the provided capability. The images were obtained using a 2 MHz, 60 degree shear wave transducer, and a 70 degree TRL probe with the same frequency.

Moreover, all rejectable flaws were correctly rejected, except for one IGSCC crack in assembly 35 that was reported with a height just under the acceptable value. One rejectable false call was generated in the same assembly.

## 2.4. Sizing Performance

The assessment of the overall sizing capability of the considered procedure was performed using the mean sizing error and the standard deviation obtained on the set of flaws in each assembly, and also globally. Only through-thickness sizing is considered in detail. Fig. 6 shows the outcome.

The averages for each assembly show both important undersizing and oversizing, independent of the flaw type present. The overall height sizing error is -0.3 mm, with a standard deviation of 3.5 mm. As the corresponding values for IGSCC defects and EDM notches are quite alike, no difference in terms of through-thickness sizing performance can be noticed. The causes for the quite moderate sizing performance are to be found in the absence of clear tip diffraction signals, and the poor accuracy of the proposed alternative, the amplitude drop method.

As far as length sizing is concerned, a far better performance was observed for non IGSCC defects : an average undersizing of about 3 mm against a value of 30 mm for IGSCC.

## 3. C/W & C/C Capability Study

### 3.1. Test Specimens

The geometry, and the material characteristics of the test assemblies presented in the cast-to-cast and cast-to wrought round-robin tests were representative for the main coolant piping of pressurized water nuclear reactors. All assemblies had diameters of about 36". The wall thickness was in the range 65-75 mm, except for a cast elbow where it was 100 mm.

Assembly 51, was a composition of three different kinds of austenitic stainless steels by two weldings : weld A connected centrifugally cast primary pipe to wrought pipe and weld B connected this wrought pipe to a statically cast 30° elbow. The latter weld presented a pipe diameter variation similar to those often encountered in actual primary piping configurations.

Assemblies 41 and 42 both consisted of several segments, bolted into a pipe configuration. Each of the segments contained a weld connecting

two different cast austenitic grain structures. For Assembly 43 the exact flaw data are not yet available. Therefore the results of this assembly are not addressed in this paper.

The set of intended flaws present in the considered assemblies contains planar surface defects such as sharp spark eroded notches and mechanical fatigue cracks, as well as sub-surface flaws, such as lack-of-fusion defects and implanted side-drilled holes.

A complete and detailed description of the assemblies and the nature and the location of each flaw will be given in (3) and (4).

### 3.2. Test Procedures

Two Belgian teams, both from AIB-Vinçotte, participated in the cast-to-cast and cast-to-wrought capability studies.

One of the teams performed an automated ultrasonic examination using a dedicated pipe inspection scanning mechanism, and a commercially available UT data recording system.

Contact 45 and 60 degree twin-crystal compression wave transducers at 1 MHz were used, together with conventional straight-beam probes. In addition, a 1 MHz 45 degree shear wave transducer was used to examine the wrought base material and the heat-affected zone. Flaw detection and sizing was performed using an ASME XI-like procedure, with a DAC reference level, which was up to now standard inspection practice in the Belgian nuclear plants.

The other team also performed an automated examination using the same versatile scanning mechanism connected to an in-house data acquisition and processing system.

In addition to contact 45 degree TRL and shear wave transducers, large crystal 1 MHz focused beam probes were used at normal incidence and at a 45 degree refracted angle. The local immersion technique was applied for transducer coupling. All flaws exceeding the local noise level were investigated, and where possible, tip diffraction signals were used for height sizing purposes.

Both teams used the same large-element 45 degree TRL probe, designed for enhanced detection capability in the far-surface region. Its better performance with respect to conventional TRL design was already demonstrated in the parametric study on the effect of the austenitic macrostructure (5) : an average SNR enhancement of 5 dB was observed.

### 3.3. Flaw Detection Capability

As for the wrought-to-wrought capability study, the quantitative assessment of the detection capability of the applied procedure was performed using the standard set of descriptive statistical parameters defined for PISC III. The results of this exercise for each of the assemblies are shown on Figs. 7-10.

Considering the complete set of intended flaws, the advanced procedure clearly shows a better performance than the ASME-like procedure. Except for weld B of Assembly 51, its FDF ranges from 75 to 90 %,

while it ranges from 50 to 75 % for the ASME-like procedure. Each of the procedures reported only one false call.

When only rejectable flaws are considered, the scores of the two procedures tend towards one another : CRF values up to 100 % are achieved. The procedure using focusing probes failed to reject only one flaw, a fatigue crack, while no false calls in rejection were generated.

The detection performance on weld B of Assembly 51 is clearly below average for both procedures. This is most probably due to the specific geometry of the outside surface in the weld region.

No clear difference in detection capability was observed between the cast-to-cast assemblies on the one hand and the cast-to-wrought assemblies on the other hand.

A more detailed analysis of the inspection results indicates two major causes for the difference in detection performance between the two procedures.

First, the ASME-like procedure only reported one lack-of-fusion defect in the weld volume, due to the limited capability of both the applied straight-beam probe and the TRL transducer for that specific kind of flaw. The focused beam probes used in the advanced procedure allowed for the detection of most of these sub-surface flaws. This is clearly illustrated on Fig. 11 : the image obtained with the 0 degree probe on a lack-of-fusion defect in assembly 51 shows a SNR of at least 16 dB, while insonifying the flaw through cast base material with the 45 degree probe still provides a SNR of 8 dB.

Second, the applied DAC threshold does not allow for the detection of planar surface flaws with a small through-thickness dimension, although in some cases they can be discriminated from the grain noise.

Supplementary aspects of detection capability were deduced through further investigation of the results of separate inspection techniques within the procedure using the grain noise as detection threshold.

Considering all planar surface flaws in the cast-to-cast assemblies, the application of only the 45 degree focusing probe from both sides of the weld provides detection of 13 out of 14 flaws, missing one acceptable EDM slot. Using only the TRL transducer allows for the detection of 11 flaws, while an unacceptable flaw is missed. Differences in SNR ranging from 0 to 6 dB, without any correlation with the defect type, are observed in favour of the focused beam probe.

For planar flaws located in the fusion line and in the heat-affected zone, insonification through the weld yields an average SNR between 2 and 3 dB higher than for an examination through the base material, for both TRL and focusing probes. Taking into account that for the applied techniques the effect of a weld in the wave path is minor, this is most probably caused by the favourable orientation of the defects for insonification through the weld.

The SNR obtained on planar defects located in the weld material is lower than for flaws in the fusion line. This might be due to either the nature of the flaws (mostly fatigue cracks) or to their orientation approximately perpendicular to the scanning surface.

The better lateral resolution of the focusing transducer provides an improved flaw characterisation capability. Fig. 12 shows the ultrasonic images of two separate planar flaws located at either side of the weld preparation : the local immersion focused probe is able to distinguish two flaws, while the TRL search unit detects one large flaw indication. In both cases insonification through cast base material is considered.

#### 3.4. Sizing Performance

The depth sizing results for the ASME-like procedure and the advanced procedure on each of the assemblies are given on the graphs of Figs. 13 and 14. Both procedures show a tendency towards oversizing. The effect is stronger for the ASME-like procedure : mean height sizing errors ranging from 0 to 7 mm or 9 % of the wall thickness are observed, compared to 2.5 mm or 3 % for the advanced procedure using tip diffraction effects. Moreover, the spread of the errors is larger for sizing based on the ASME method.

Figs. 15 and 16 provide more information about the influence of the flaw type on through-thickness sizing for each of the procedures.

The ASME-like procedure strongly oversized the so-called PISC type "A" defects. Obviously, the amplitude drop method generates flaw heights corresponding to the large beam width of the applied TRL search units. The advanced procedure yields far better results on this type of defect, through the interpretation of tip diffraction signals generated almost exclusively by the focusing probes. A good illustration of the accurate depth sizing obtained with this technique is shown on Fig. 17. Both tip and corner echoes of a 20 mm deep EDM notch in a cast assembly are clearly visible. The ultrasonic image of the same flaw provided by the TRL probe is given for comparison.

Both procedures have undersized the mechanical fatigue cracks in the cast assemblies. A 13 mm deep fatigue crack located in the weld of assembly 41 generated the largest sizing error for the advanced procedure. As the crack could hardly be discriminated from the grain noise with any of the applied probes, obviously proper sizing was not possible.

The overall sizing performance of both procedures is deteriorated by the rather arbitrary results on sub-surface lack-of fusion defects with a very small through-thickness dimension. This is probably due to the fact that the applied inspection techniques were designed for optimal performance on crack-like flaws in the far-surface region of the components.

#### 4. Conclusions and Recommendations

Due to the nature of austenitic material, caution must always be taken in transposing results obtained on specific assemblies. Nevertheless, some important conclusions can be deduced from the Belgian work.

The examination of austenitic stainless steel welds in auxiliary piping with contact TRL and shear wave transducers provides an excellent detection capability.

However, height sizing has to be improved. Therefore other techniques have to be implemented, that fully exploit the advantages of crack tip diffraction effects.

For planar surface-breaking flaws in thick cast piping, such as the main coolant piping, automatically scanned large 45 degree TRL search units demonstrated a detection capability almost as good as the focusing probes, provided that noise level detection is used. Thus, scanning the large immersion devices in normal detection mode might be avoided, which is favourable with respect to inspection duration and site conditions with limited weld access.

On the other hand, it was also clearly demonstrated that the application of large diameter focused beam probes, in combination with the tip diffraction method, significantly improves characterization and height sizing of flaws.

Finally, it is important to mention that in the framework of the evolution towards inspection qualification, the Belgian utility has shown large interest in the results of the cast-to-cast and cast-to-wrought capability studies. As a consequence of its good overall performance, AIB-Vinçotte was asked to prepare the field implementation of the applied automated detection and sizing techniques.

- 
1. PISC III Report N°33 "Report on the Evaluation of the Inspection Results of the Wrought to Wrought PISC III Assemblies 31, 32, 33, 34, 35, 36", Draft version, 1994
  2. PISC III Report N°21 (EUR 15559 EN), "PISC III Rules for the Evaluation of the RRT Results", 1993
  3. PISC III Report N°34 "Report on the Evaluation of the Inspection Results of the Cast to Cast PISC III Assemblies 41, 42, and 43", to be published
  4. PISC III Report N°35 "Report on the Evaluation of the Inspection Results of the Wrought to Cast PISC III Assembly 51", to be published.
  5. G. Maes, B. Hansoul, Ph. Dombret, "The PISC Parametric Study on the Effect of Cast Austenitic Steel Macrostructure on the Capability of Ultrasonic Examination", 12th Int. Conference on NDE in the Nuclear and Pressure Vessel Industry, Philadelphia (PA), 1993

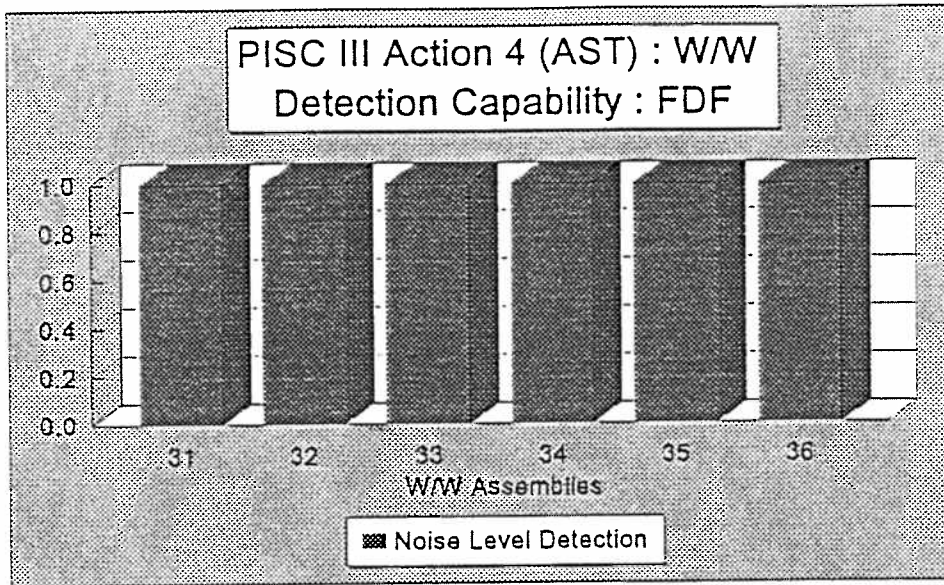


Figure 1 : FDF (Flaw Detection for all Flaws) obtained for each assembly (FDF is the ratio of the number of detected flaws by the total number of flaws)

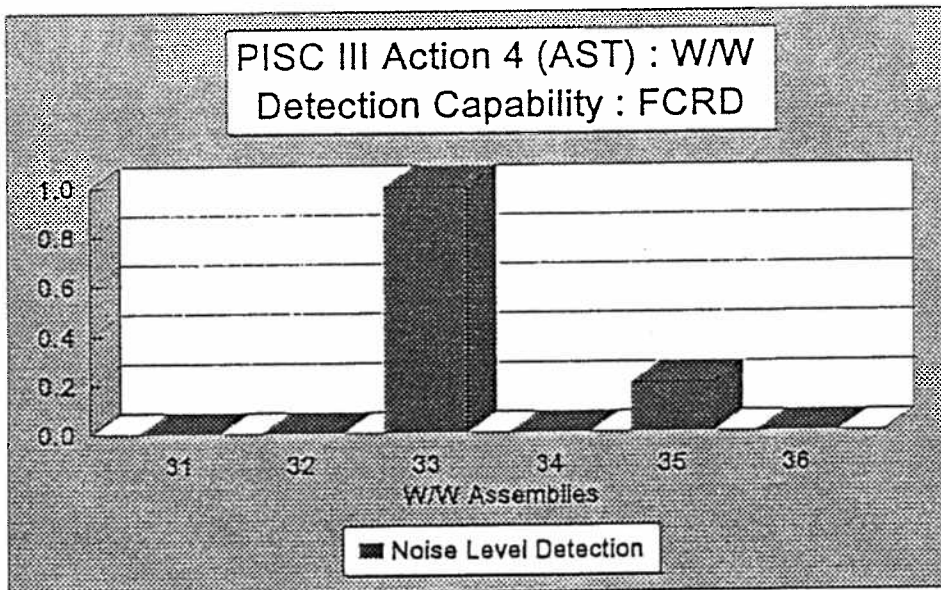


Figure 2 : FCRD (False Call Rate in Detection) obtained for each assembly (FCRD is the ratio of the number of detected non-existing flaws by the total number of detected flaws)

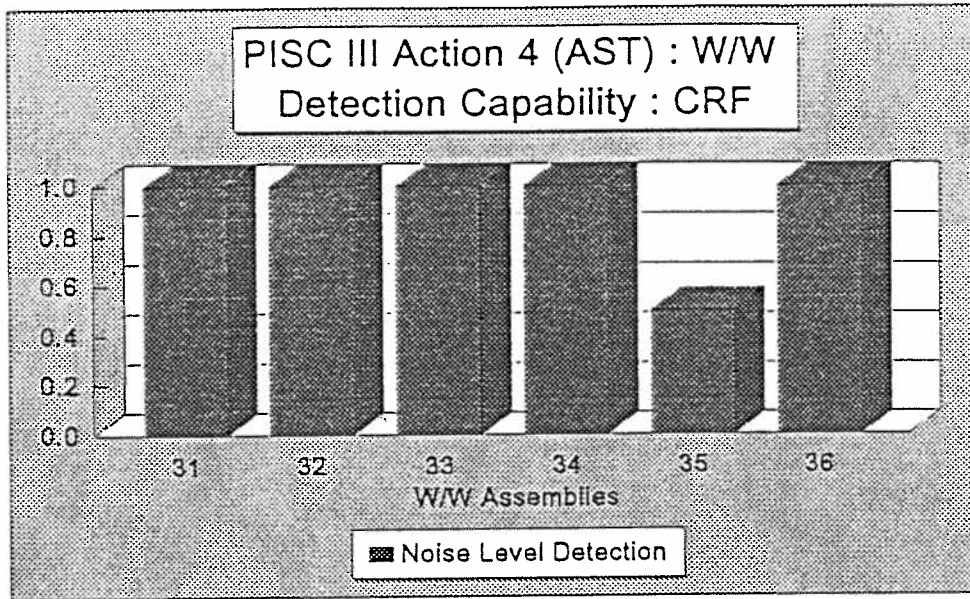


Figure 3 : CRF (Correct Rejection of Flaws) obtained for each assembly (CRF is the ratio of the number of correctly rejected flaws by the total number of rejectable flaws)

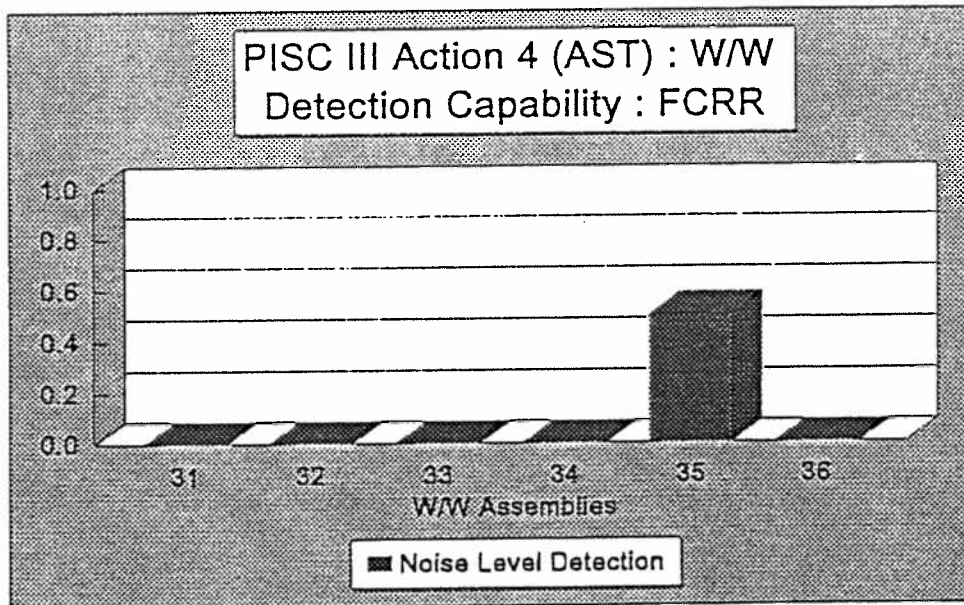


Figure 4 : FCRR (False Call Rate in Rejection) obtained for each assembly (FCRR is the ratio of the number of false rejections by the total number of rejected flaws)

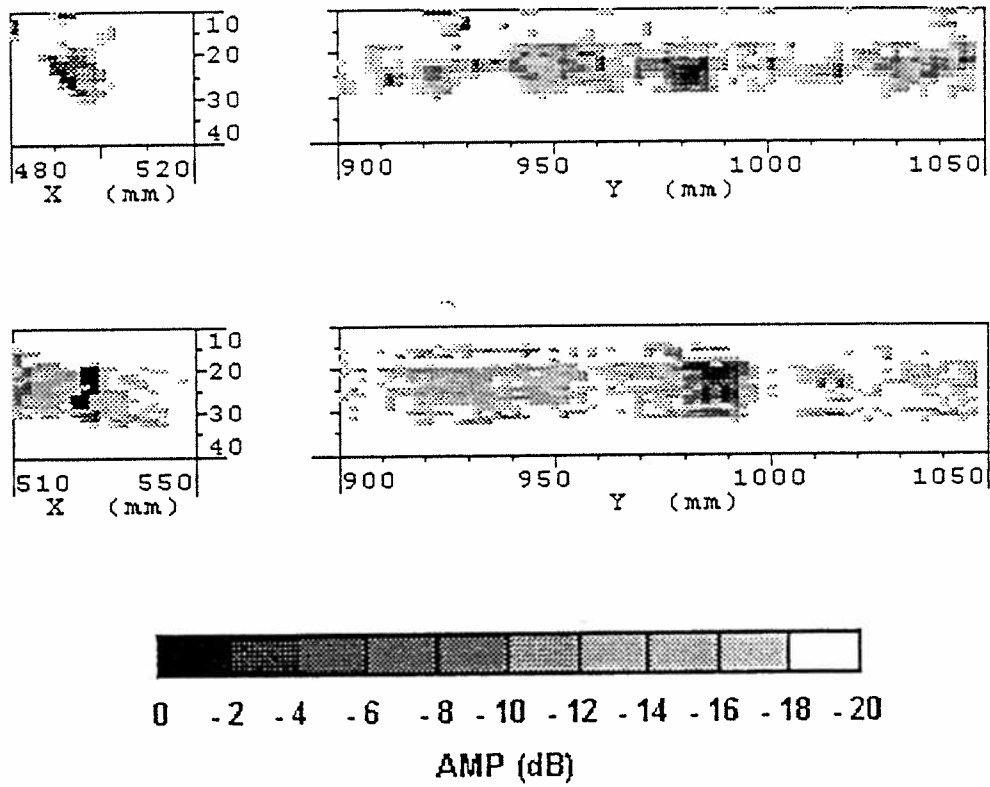


Figure 5 : B-scan and D-scan views of 0.4 mm deep EDM notch ; 2 MHz 60° shear wave probe (top), and 2 MHz 70°TRL probe (bottom)

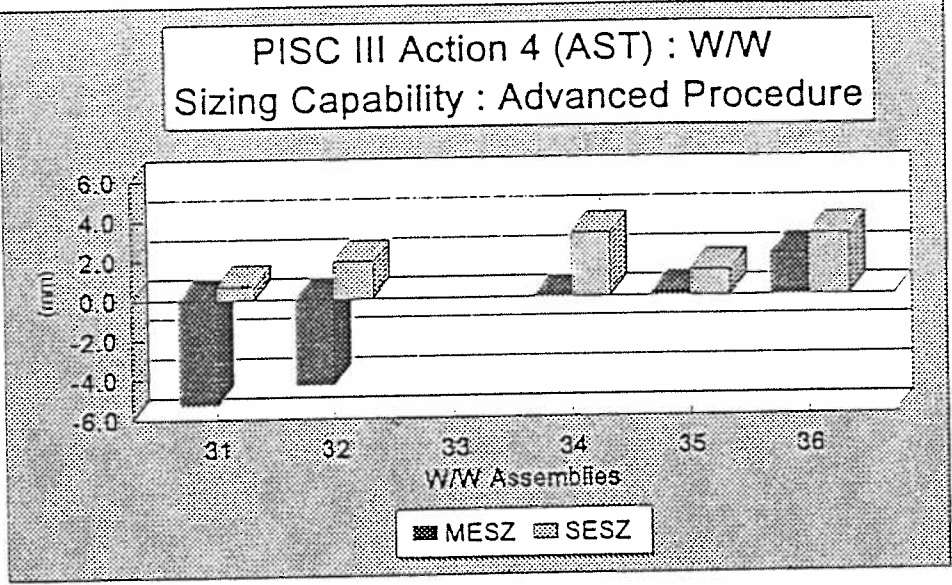


Figure 6 : Average values (MESZ) and standard deviations (SESZ) of height sizing errors in wrought assemblies

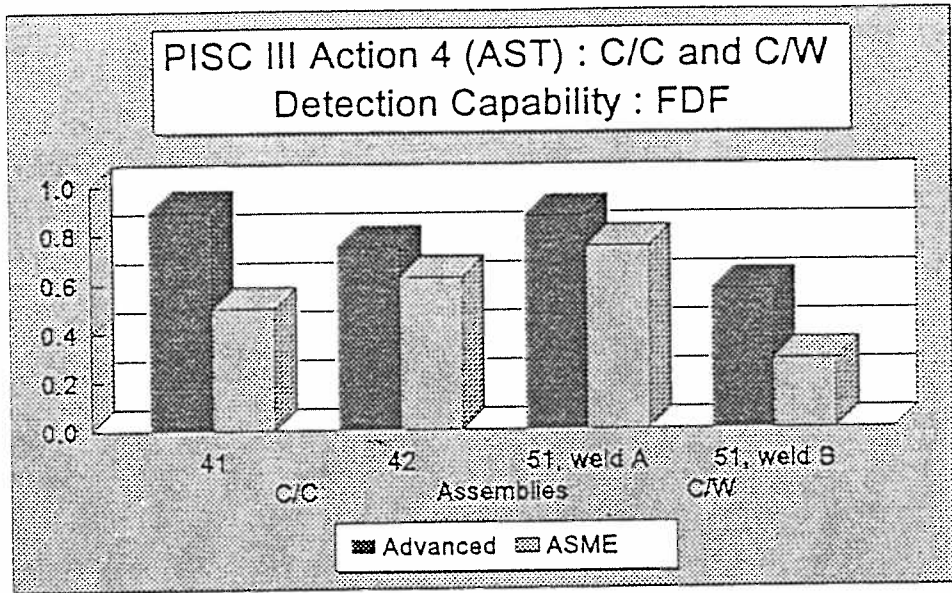


Figure 7 : FDF (Flaw Detection for all Flaws) obtained for each assembly

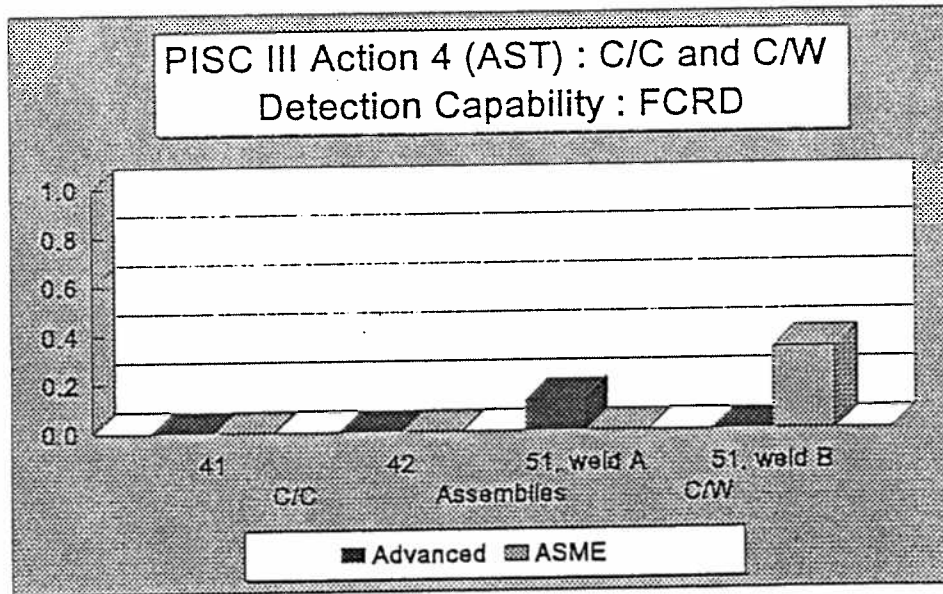


Figure 8 : FCRD (False Call Rate in Detection) obtained for each assembly

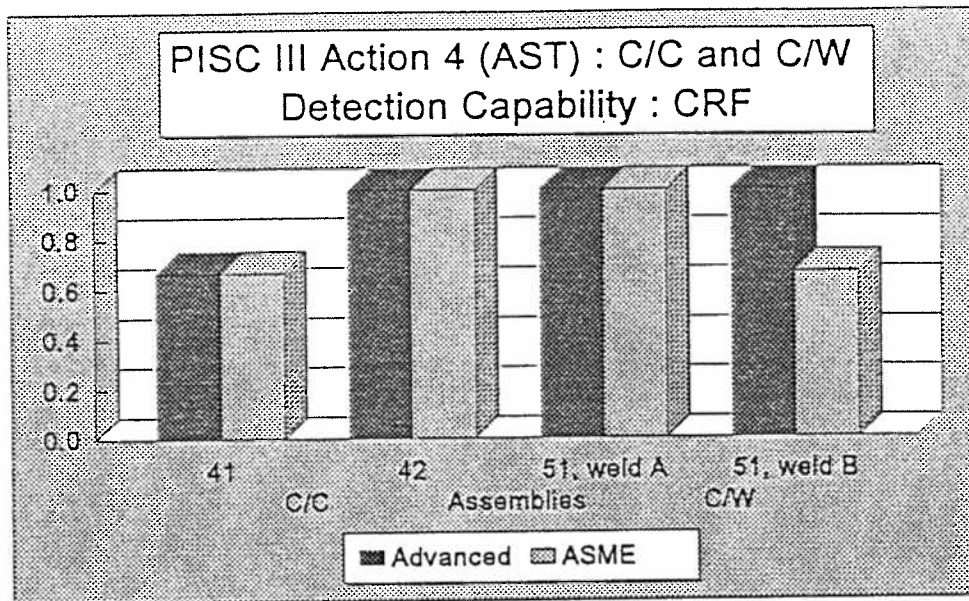


Figure 9 : CRF (Correct Rejection of Flaws) obtained for each assembly

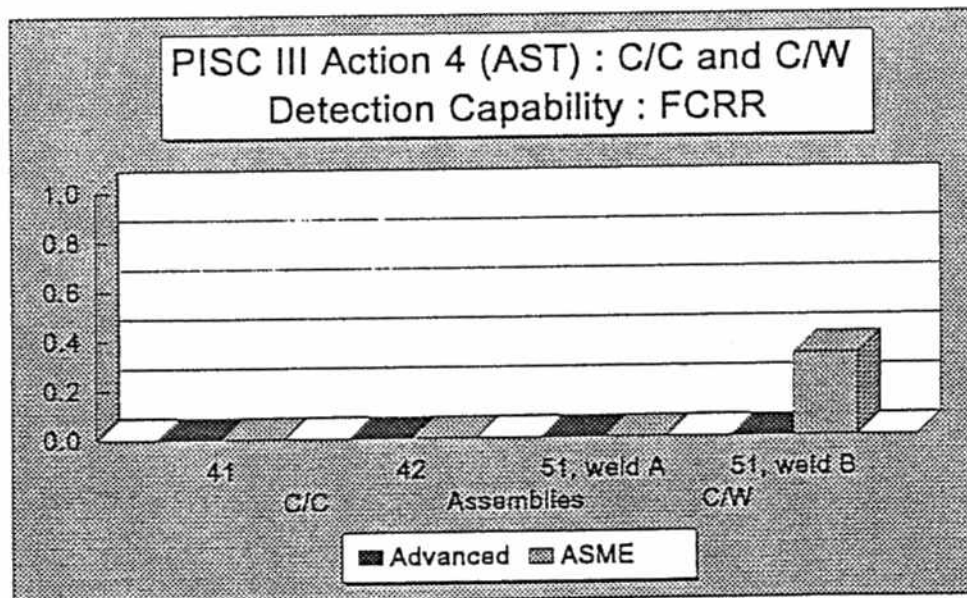


Figure 10 : FCRR (False Call Rate in Rejection) obtained for each assembly

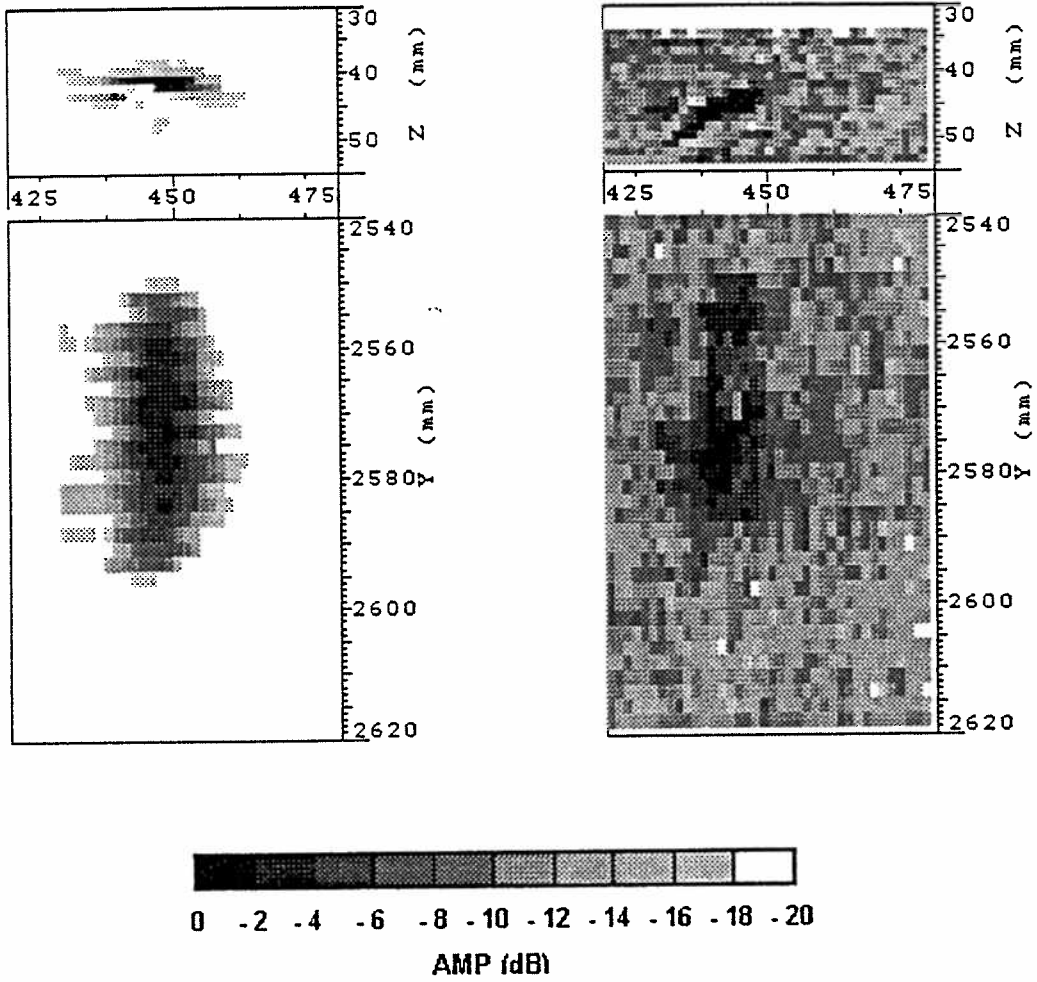


Figure 11 : B-scan (top) and C-scan (bottom) views of a lack of fusion defect in the weld volume ; results from 1 MHz 0°L probe (left) and 45°L probe (right)

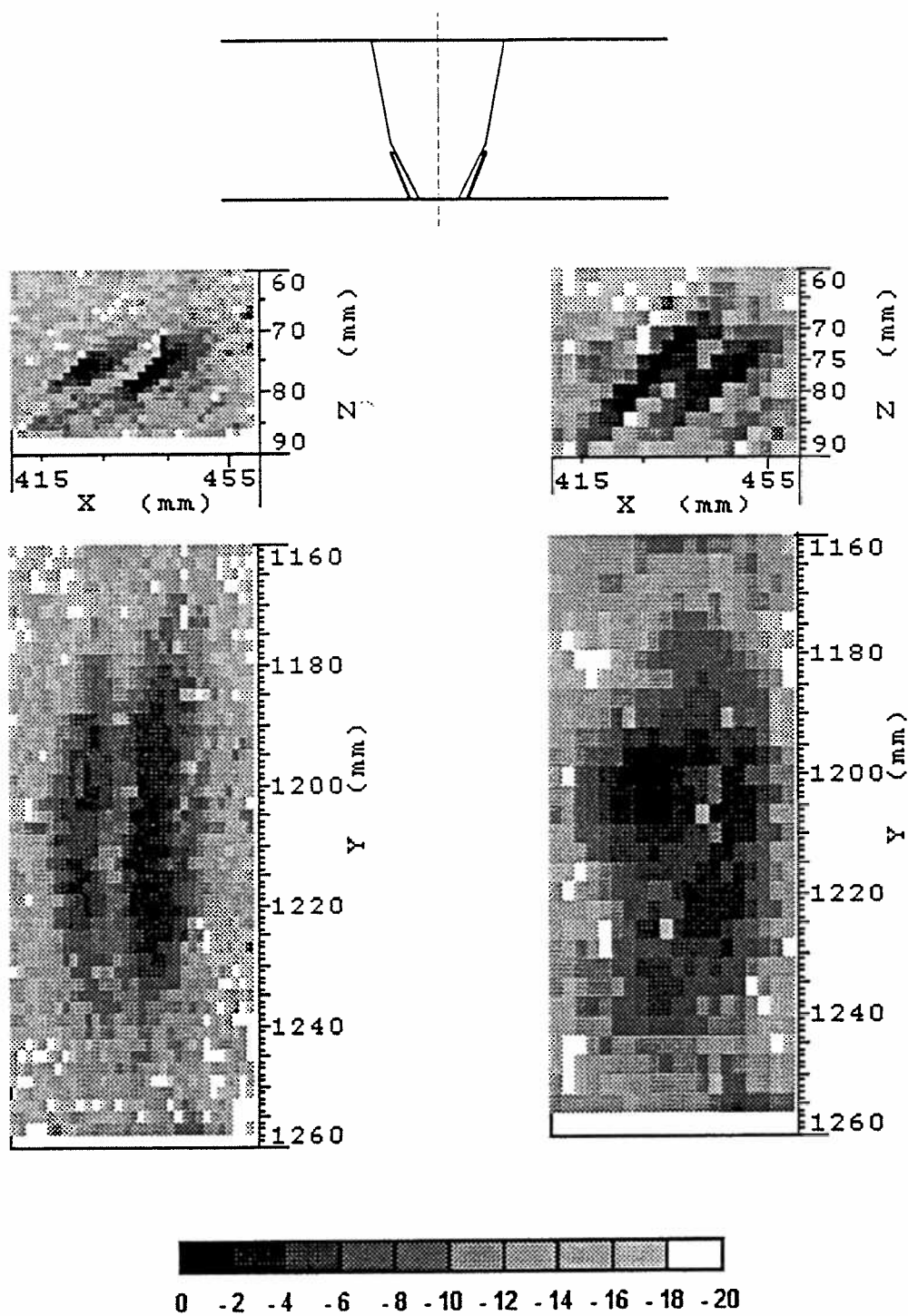


Figure 12 : B-scan (top) and C-scan (bottom) views of 2 "type A" defects in the weld preparation ; results from 1 MHz focussed probe (left) and 1 MHz TRL transducer (right)

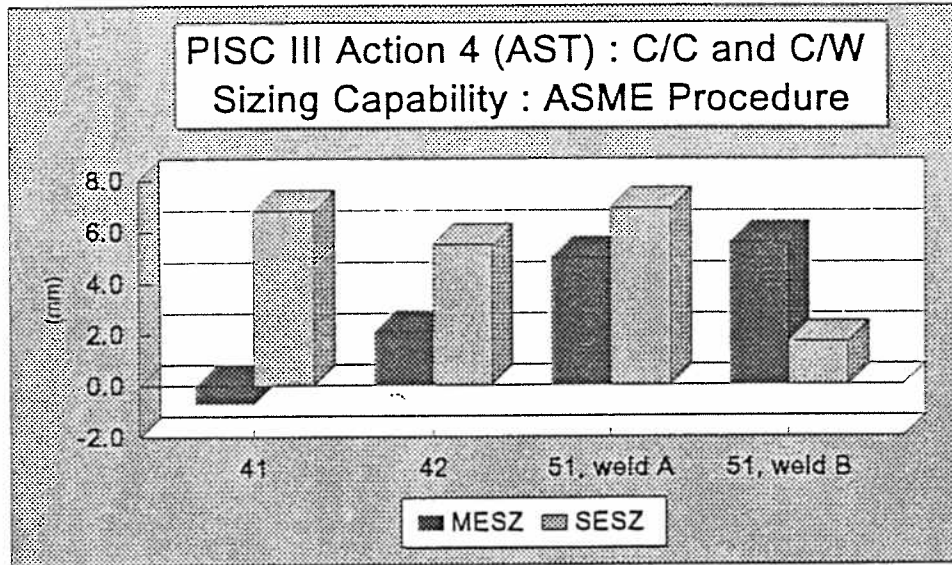


Figure 13 : Average values (MESZ) and standard deviations (SESZ) of height sizing errors for the ASME-like procedure

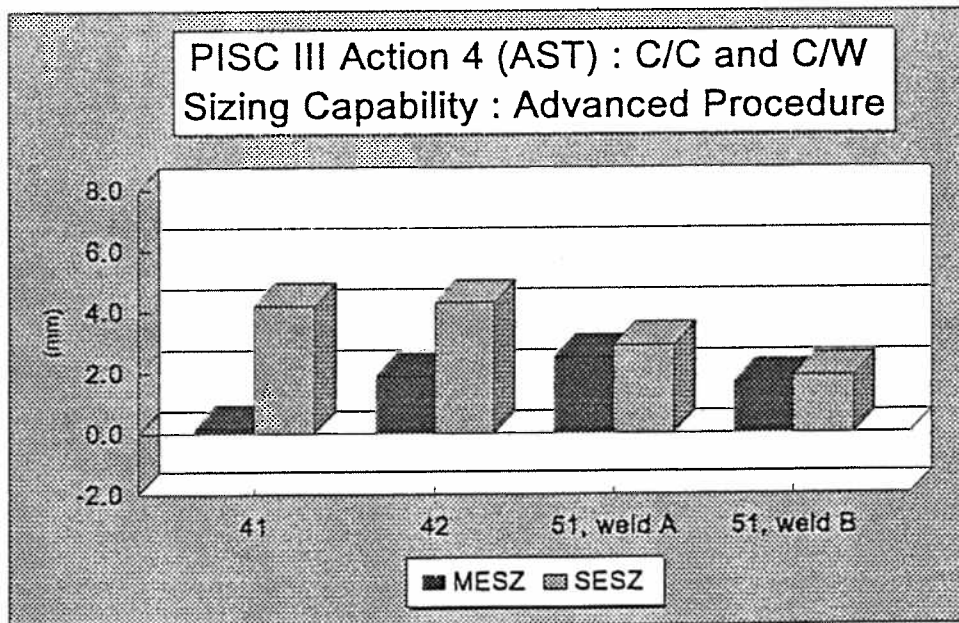


Figure 14 : Average values (MESZ) and standard deviations (SESZ) of height sizing errors for the advanced procedure

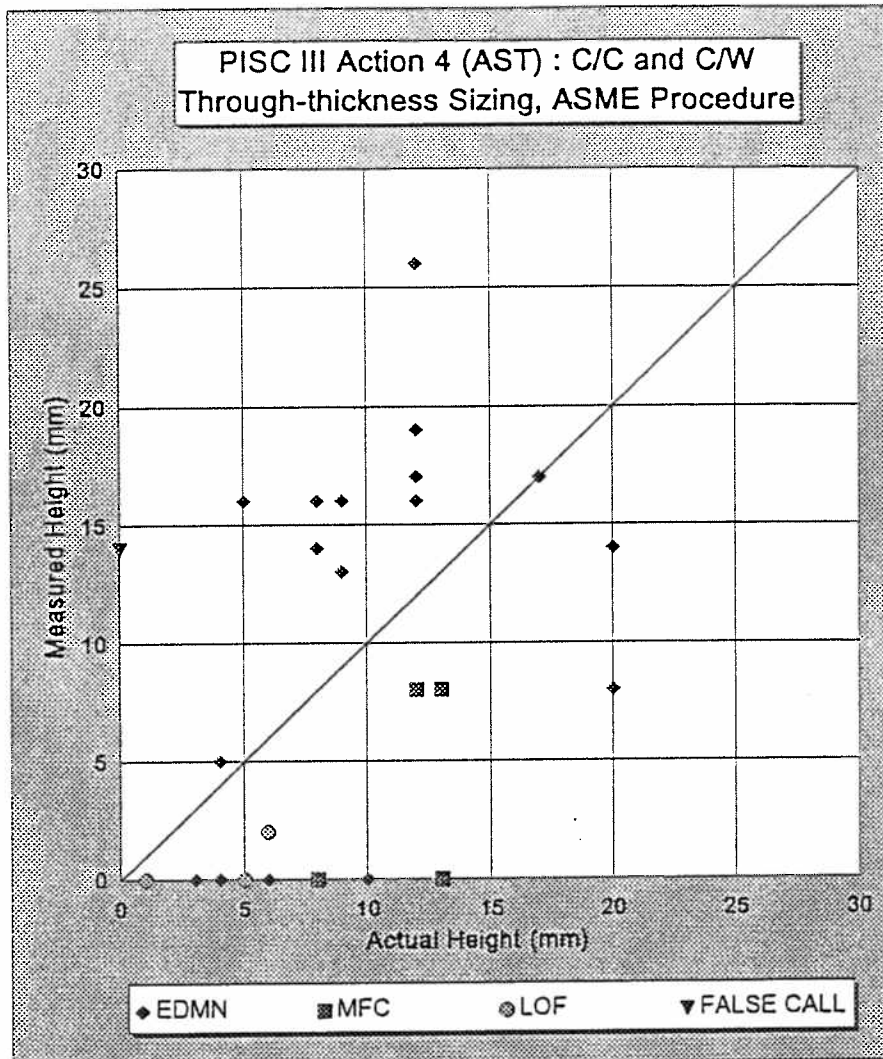


Figure 15 : Measured vs. actual height for individual flaws, results for the ASME-like procedure

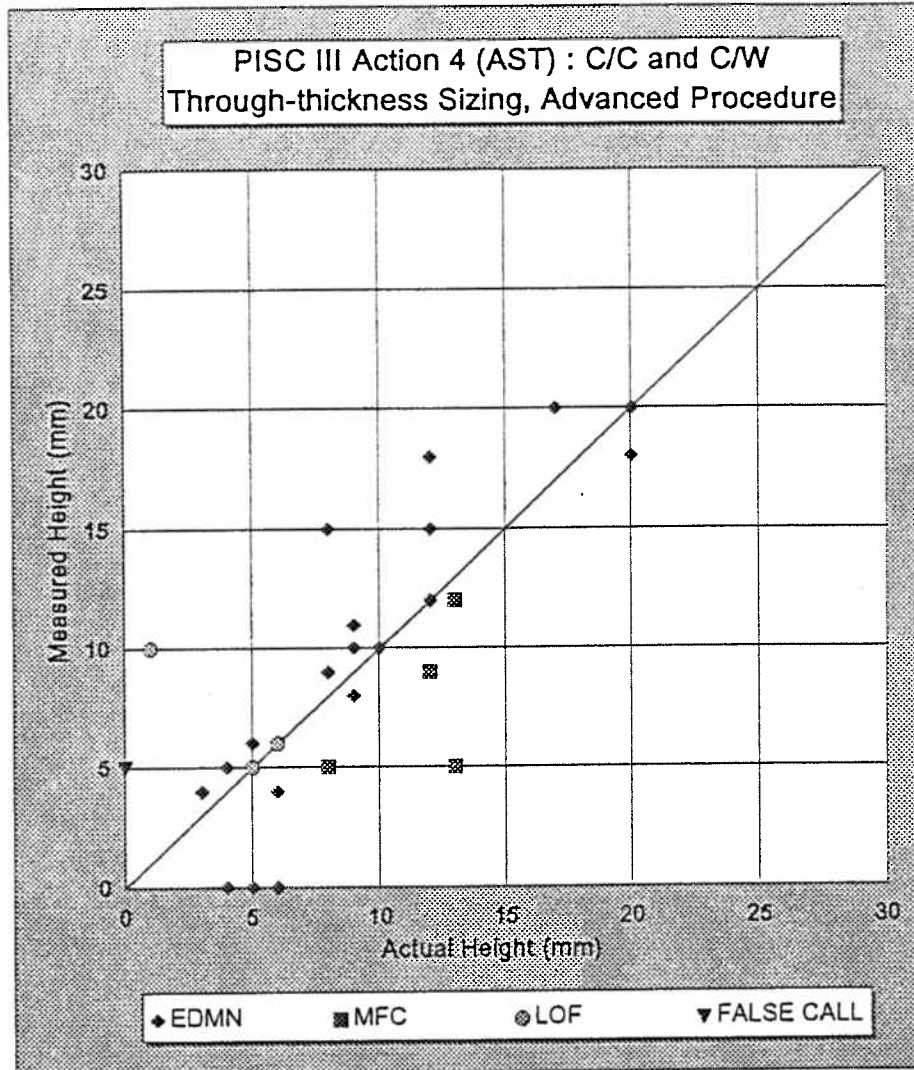


Figure 16 : Measured vs. actual height for individual flaws, results for the advanced procedure

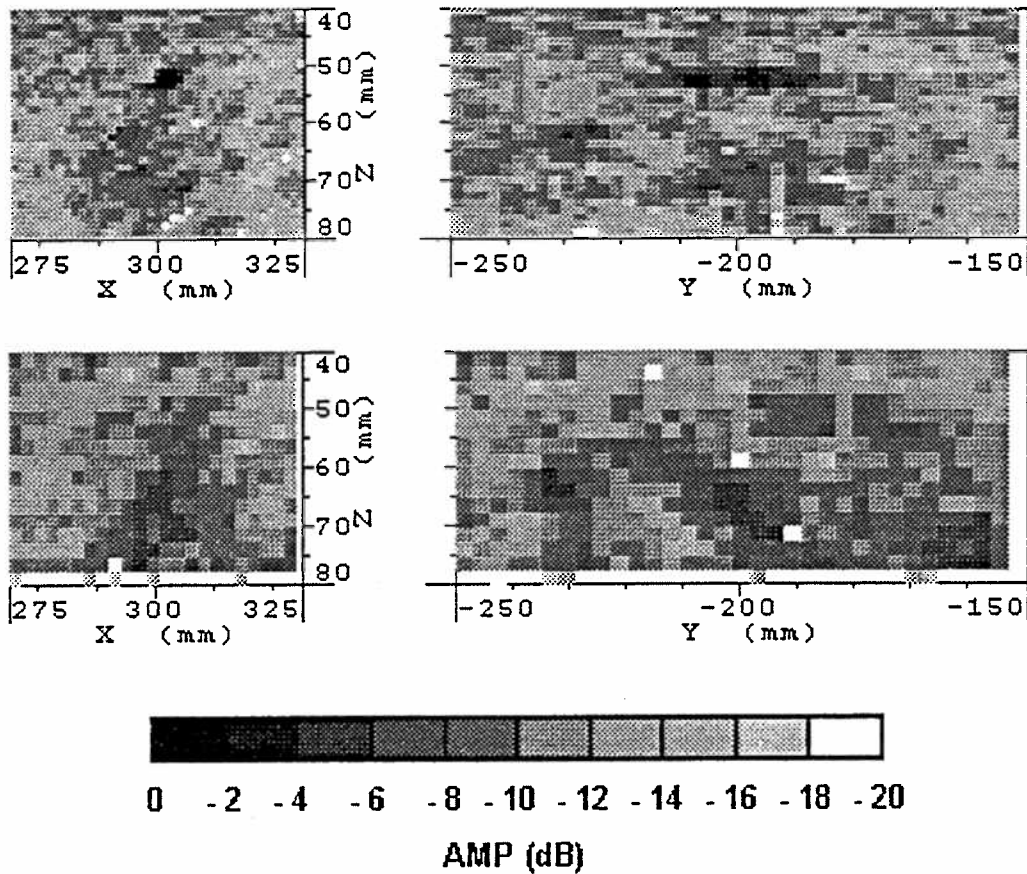


Figure 17 : B-scan (left) and D-scan (right) views of planar surface flaw ; sizing with 1 MHz focussed probe (top), and 1 MHz 45°TRL probe (bottom)